

Received:  
30 November 2016

Revised:  
8 March 2017

Accepted:  
14 March 2017

<https://doi.org/10.1259/bjr.20160901>

Cite this article as:

Benson DG, Schiebler ML, Repplinger MD, François CJ, Grist TM, Reeder SB, et al. Contrast-enhanced pulmonary MRA for the primary diagnosis of pulmonary embolism: current state of the art and future directions. *Br J Radiol* 2017; **90**: 20160901.

## REVIEW ARTICLE

# Contrast-enhanced pulmonary MRA for the primary diagnosis of pulmonary embolism: current state of the art and future directions

<sup>1</sup>DONALD G BENSON, MD, <sup>1</sup>MARK L SCHIEBLER, MD, <sup>1,2</sup>MICHAEL D REPPLINGER, MD, PhD,  
<sup>1</sup>CHRISTOPHER J FRANÇOIS, MD, <sup>1,3,4</sup>THOMAS M GRIST, MD, <sup>1,2,3,4,5</sup>SCOTT B REEDER, MD, PhD  
and <sup>1,3,6</sup>SCOTT K NAGLE, MD, PhD

<sup>1</sup>Department of Radiology, University of Wisconsin—Madison, Madison, WI, USA

<sup>2</sup>Department of Emergency Medicine, University of Wisconsin—Madison, Madison, WI, USA

<sup>3</sup>Department of Medical Physics, University of Wisconsin—Madison, Madison, WI, USA

<sup>4</sup>Department of Biomedical Engineering, University of Wisconsin—Madison, Madison, WI, USA

<sup>5</sup>Department of Medicine, University of Wisconsin—Madison, Madison, WI, USA

<sup>6</sup>Department of Pediatrics, University of Wisconsin—Madison, Madison, WI, USA

Address correspondence to: Dr Scott K Nagle

E-mail: [SNagle@uwhealth.org](mailto:SNagle@uwhealth.org)

## ABSTRACT

CT pulmonary angiography (CTPA) is currently considered the imaging standard of care for the diagnosis of pulmonary embolism (PE). Recent advances in contrast-enhanced pulmonary MR angiography (MRA) techniques have led to increased use of this modality for the detection of PE in the proper clinical setting. This review is intended to provide an introduction to the state-of-the-art techniques used in pulmonary MRA for the detection of PE and to discuss possible future directions for this modality. This review discusses the following issues pertinent to MRA for the diagnosis of PE: (1) the diagnostic efficacy and clinical effectiveness for pulmonary MRA relative to CTPA, (2) the different pulmonary MRA techniques used for the detection of PE, (3) guidance for building a clinical service at their institution using MRA and (4) future directions of PE MRA. Our principal aim was to show how pulmonary MRA can be used as a safe, effective modality for the diagnosis of clinically significant PE, particularly for those patients where there are concerns about ionizing radiation or contraindications/allergies to the iodinated contrast material.

## INTRODUCTION

Pulmonary embolism (PE) is the third leading cause of acute cardiovascular death in the world, following myocardial infarction and stroke.<sup>1,2</sup> PE is fatal in up to 30% of affected patients if not treated promptly, necessitating a quick, accurate diagnosis.<sup>3,4</sup>

Following the completion of the large, multicentre PLOPED II study comparing the diagnostic efficacy of CT pulmonary angiography (CTPA), nuclear medicine ventilation/perfusion (V/Q) scintigraphy and conventional angiography, CTPA has become the “imaging standard of care” for diagnosis of PE.<sup>5</sup> Moreover, CTPA can be performed and interpreted rapidly, resulting in its widespread use in the emergency setting.

CTPA has its limitations, however. There are increasing concerns about the effects of ionizing radiation, particularly for younger females.<sup>6–9</sup> Also, some patients

have contraindications to iodinated contrast, including those with renal failure (estimated glomerular filtration rate <30) or a history of allergic or anaphylactoid reaction to the contrast material.

MR angiography (MRA) can also be used for the diagnosis of PE and does not require either iodinated contrast or ionizing radiation. Historically, MRA has been limited by longer acquisition times, limited volumetric coverage and lower spatial resolution than CTPA. More recent technological advances including view sharing, parallel imaging and time-resolved MRA, however, have shortened the acquisition times and have led to increased use of MRA for the primary diagnosis of PE.<sup>10</sup>

The purpose of this review was to provide an update on the current state of the art of pulmonary MRA for the diagnosis of clinically significant PE, including its limitations and potential future developments.

## DIAGNOSTIC EFFICACY VS CLINICAL EFFECTIVENESS

With improvements in MR technology and pulmonary MRA protocols, there has been increasing interest in comparing this modality with the current diagnostic imaging standard, CTPA. Comparisons of this nature are challenging, and ultimately the decision to choose one modality over another is multifactorial. Crucially, superior diagnostic efficacy does not necessarily result in improved clinical outcomes.<sup>11,12</sup>

The diagnostic efficacy of an imaging examination is its ability to distinguish normal from diseased patients. Efficacy is typically quantified by standard measures such as sensitivity, specificity and accuracy.<sup>11,13</sup> Alternatively, the clinical effectiveness of an imaging examination describes the utility of a diagnostic examination in guiding treatment decisions that affect patient outcomes. Clinical effectiveness can be assessed by comparing outcomes between groups of patients who were treated based on the findings of the different diagnostic examinations.<sup>12</sup>

Most studies that compare different diagnostic imaging examinations focus on diagnostic efficacy. Clearly, diagnostic efficacy is important for treatment decisions. However, other factors such as safety, incidental findings or overdiagnosis of clinically occult disease may confound the clinical situation. Incidental findings, for example, may lead to additional testing and unnecessary treatments. Positive findings may prompt the referring physician to prescribe an unnecessary treatment that may lead to severe side effects. This is referred to as “overdiagnosis”.

A relevant example of possible overdiagnosis is the subsegmental pulmonary embolus (SSPE). As recent studies have shown, SSPE may not be clinically significant, and the treatment (anti-coagulation) may lead to adverse events.<sup>14–16</sup> On the other hand, many authors suggest that all SSPE may be significant.<sup>17,18</sup> Further work in this area is needed to determine the appropriate treatment strategies for SSPE.

The largest efficacy study assessing the accuracy of pulmonary MRA for the detection of PE was PIOPED III.<sup>19</sup> In this study, 371 patients were evaluated with contrast-enhanced MR angiography (CE-MRA). Pulmonary MRA was compared with several reference standards for the diagnosis or exclusion of PE. In this study, 25% of pulmonary MRA examinations were found to be technically inadequate. Including these inadequate studies, only 57% of patients with known PE were identified with MRA. Excluding technically inadequate studies, the sensitivity of MRA for detecting PE was 78%, with a specificity of 99%. Technical inadequacy varied significantly by study site, ranging from 11% to 51%, possibly related to differing levels of experience among institutions. The majority of the inadequate studies were caused by poor arterial opacification and motion artefact.<sup>20</sup> Further, the technology and methodology used in the PIOPED II study is now over a decade old, including a lack of consistent two-dimensional (2D) parallel imaging at many sites. Given major advances in hardware (gradients, receiver chain, radiofrequency coils), software (parallel imaging algorithms) and bolus injection methods, the results of PIOPED III are likely outdated.

Since PIOPED III, there has been one study evaluating the clinical effectiveness of pulmonary MRA for the primary diagnosis of PE.<sup>10</sup> That retrospective study of 190 patients evaluated reported a negative-predictive value for MRA of 97% at 3 months and 96% at 1 year of follow-up, similar to literature-reported values for CTPA. Furthermore, in contrast to the PIOPED III study, the real-world technical success rate of MRA was high, with 97% of the examinations being of diagnostic quality. This difference can be attributed to several factors: (a) improved, consistent 2D parallel imaging; (b) dilution of the contrast to prolong the bolus for better arterial opacification; and (c) acquisition of multiple vascular phases to improve the likelihood of acquiring images without motion artefact. It is doubtful that a study the size of PIOPED III will be repeated to further assess the diagnostic efficacy of pulmonary MRA using CTPA as a reference standard, but it is feasible for other studies to prospectively evaluate patient outcomes.

## MRI TECHNIQUES USED FOR PULMONARY EMBOLISM DETECTION

The feasibility of detecting PE using MRI was first demonstrated in the early 1980s.<sup>21</sup> Improved protocols using both spin-echo and gradient-echo techniques in the early 1990s were used to obtain sensitivities and specificities that were similar to ventilation perfusion scintigraphy for the detection of PE.<sup>22–24</sup> Gadolinium-enhanced pulmonary MRA to evaluate for PE was first performed in the late 1990s.<sup>25,26</sup> With the introduction of multidetector CT, CT angiography became the standard of care for detecting PE following the large PIOPED II study in the early 2000s.<sup>5</sup> The subsequent PIOPED III study performed from 2006 to 2008 is the largest study to date comparing MRA with CTPA.<sup>19</sup> Based on the results of that study, the authors recommended that pulmonary MRA only be used to diagnose PE at institutions with adequate experience in acquiring and interpreting these studies and only in patients where other examinations are contraindicated.<sup>19,20</sup> New advances in MRI technology and clinical experience since PIOPED III have made MRI an increasingly viable tool to evaluate for PE in patients where there are concerns for exposure to ionizing radiation or iodinated contrast agents.

### Contrast-enhanced MR angiography

The most important sequences in a pulmonary CE-MRA protocol are those acquired after the administration of an i.v. contrast agent using a rapid three-dimensional (3D) spoiled gradient-echo sequence. The goal in the vascular phases of pulmonary CE-MRA, such as in CTPA, is to enhance the pulmonary arterial system to facilitate identification of intraluminal filling defects. The quality of the images obtained during these acquisitions depends on a variety of factors.

Since the time of the PIOPED III study, there has been increasing availability of 2D autocalibrated parallel imaging<sup>27,28</sup> in both phase-encoding directions. This has improved spatial resolution while simultaneously enabling shorter acquisition times. The shorter breath-holds have resulted in decreased motion artefact. Diagnostic images can be obtained using both 1.5-T and 3.0-T magnets with the potential for higher resolution on a 3.0-T scanner.<sup>29</sup>

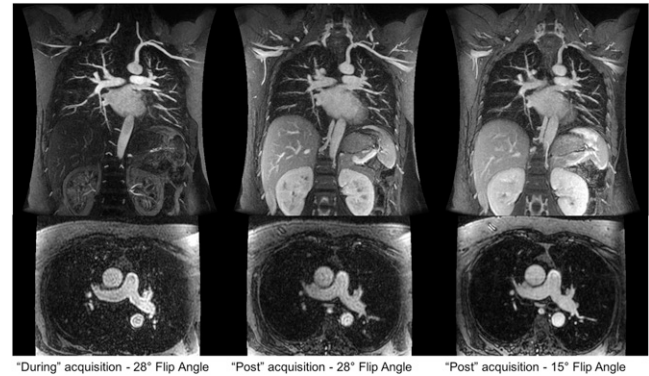
Our institution uses  $0.1\text{-mmol kg}^{-1}$  gadobenate dimeglumine (Multihance; Bracco Inc., NJ), but other gadolinium-based contrast agents (GBCAs) can be used. The intravascular agent gadofosveset trisodium (Ablavar; Lantheus Medical Imaging, Inc., North Billerica, MA) is no longer available, but the ultra-small, superparamagnetic iron oxide (USPIO) particle ferumoxytol can be used as an alternative intravascular agent. This agent is useful in patients with contraindications to GBCA administration. While it can be injected as a bolus, the Food and Drug Administration (FDA) recommends a slow infusion of diluted ferumoxytol.<sup>30</sup> Finn<sup>31</sup> at the University of California Los Angeles Medical centre has created an online registry for all patients who have had ferumoxytol administered as part of an MRA. To date, there have been no adverse events reported in over 217 cases.<sup>32</sup>

The injection protocol is critical to obtain high-quality images. Fluoroscopic triggering using real-time 2D bolus tracking imaging<sup>33</sup> can reduce the overall scan time without injecting additional contrast. Ideally, the GBCA concentration within the pulmonary arteries should be constant throughout the entire acquisition of the  $k$ -space data. Shortening the time of the  $k$ -space acquisition can help. This is accomplished by using 2D parallel imaging, minimizing repetition time and using “corner cutting”, a method whereby only an elliptical region in the phase encode dimensions of  $k$ -space is measured, with the corners of  $k$ -space then filled with zeroes during post-processing.<sup>34</sup> Even with these advances, using a non-diluted contrast bolus can lead to bolus times of  $<10$  s in patients who are small, while typical acquisition times are often 15–20 s. Diluting the bolus with normal saline to a total volume of 30 ml and injecting at a rate of  $1.5\text{ ml s}^{-1}$  extends the bolus duration to 20 s. This leads to more uniform contrast concentration throughout the pulmonary arteries during the  $k$ -space acquisition, resulting in less blurring and dynamic contrast concentration-related artefacts. A more compact, non-diluted contrast bolus could be used to decrease venous contamination if timed properly. However, multiplanar reformatted images obtained from the 3D acquisitions allow for anatomic separation of the pulmonary arteries and veins and make venous contamination less of an issue.

Additional vascular phase acquisitions can be obtained with a few additional breath-holds (Figure 1). Since patients tend to have greater difficulty holding still and completing a breath-hold during the contrast injection, these additional acquisitions often show decreased motion artefact and improved depiction of the pulmonary arteries. Furthermore, while rarely necessary, it is possible to perform a second injection if the image quality of the vascular acquisitions is poor owing to breathing motion or other technical problems, unlike with CTPA. An additional post-contrast  $T_1$  weighted spoiled gradient recalled echo (SGRE) acquisition with fat saturation can be used to assess for other pathology in the mediastinum and chest wall.

Depending on the timing of the image acquisition relative to the contrast bolus, enhancement of the lung parenchyma is occasionally seen on the arterial phase images. In these cases, perfusion defects can appear, guiding the search for possible PE (Figure 2).

Figure 1. Coronal three-dimensional spoiled gradient recalled echo with axial reconstructions: multiple acquisitions can be performed following the administration of the i.v. contrast. Here, the first acquisition is performed during the contrast injection immediately followed by two additional acquisitions. The later acquisition uses a lower flip angle owing to the decreased gadolinium-based contrast agent concentration resulting in a decreased Ernst angle of the enhanced vessels.



Time-resolved contrast-enhanced perfusion imaging  
Dedicated perfusion imaging can also be performed using dynamic contrast-enhanced MRI sequences that can evaluate the perfusion of the lung parenchyma both qualitatively and quantitatively.<sup>35–37</sup> The presence of a perfusion defect may not only help identify a PE but may provide additional information regarding its functional significance (Figure 3).

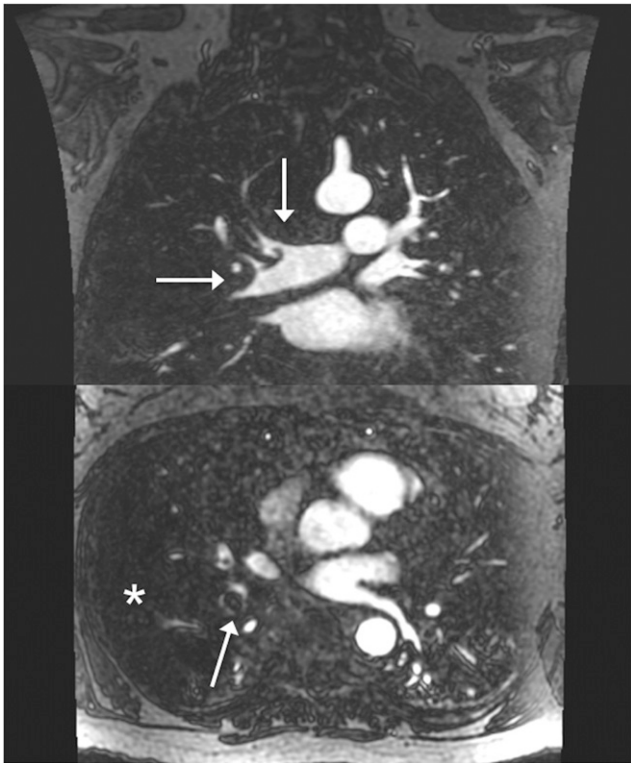
Following the administration of a GBCA, a rapid volumetric imaging sequence (e.g. 3D SGRE time-resolved MRI) can be used to assess the pulmonary perfusion either during a long breath-hold or during shallow free breathing. The use of parallel imaging and view sharing allows for temporal resolution of approximately 1 s. Qualitatively, perfusion defects can be identified by using the imaged phase on which the normal lung parenchyma is maximally enhanced or by using a maximum intensity projection through the time dimension. Correlation with pulmonary MRA can be used to identify whether or not a PE is the cause of a perfusion defect.<sup>38</sup>

For quantitative purposes, dynamic physiologic parameters such as pulmonary blood flow, pulmonary blood volume and mean transit time can be calculated using an arterial input function measured in either the main pulmonary artery or in the right ventricle.<sup>39</sup> Unfortunately, unlike the iodinated contrast material on CTPA images, the signal intensity derived from GBCAs using MRI is not linearly dependent on contrast material concentration and absolute quantitation is very challenging.<sup>40</sup>

#### Non-contrast MR angiography

The earliest attempts to evaluate for PE using MRI were made at a time when GBCAs were being used only sparingly. The performance of the non-contrast methods developed at that time has been surpassed by CE-MRA, but there are still many situations in which these methods are useful, most notably if the patient has a gadolinium contrast allergy or is pregnant. The most widely used non-contrast MRA method for assessing

Figure 2. Coronal three-dimensional gadolinium-based contrast agent with axial reconstructions: extensive pulmonary embolism (arrows) saddles the branching of the right upper lobar and interlobar pulmonary arteries and extends distally. There is also a large perfusion defect (asterisk).

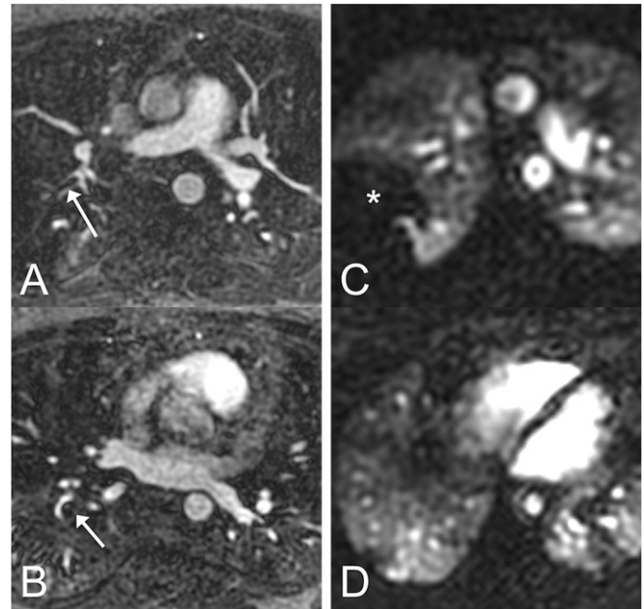


pulmonary arteries is the bright blood balanced steady-state free-precession (bSSFP) sequence (Figure 4). Some studies have shown that non-contrast bSSFP examinations perform comparably with CE-MRA when evaluating the central and lobar pulmonary arteries.<sup>41,42</sup> There are other non-contrast techniques, such as the quiescent-interval slice-selective method,<sup>43</sup> which are being applied to pulmonary MRA; however, CE-MRA remains superior in evaluating the smaller vessels.

Black blood spin-echo techniques can be useful in the setting of chronic pulmonary artery hypertension,<sup>44</sup> but are not routinely used in the evaluation of pulmonary embolus owing to the low signal of most emboli. Standard non-contrast MRA techniques such as time of flight and phase contrast are of limited utility in assessing the pulmonary arteries secondary to breathing and cardiac motion.

There are additional non-contrast techniques that have not been formally assessed for detection of pulmonary emboli. Electrocardiogram-gated 3D half-Fourier fast spin-echo sequences that use the difference in signal intensity within a vessel during systole and diastole have also been described as a possible non-contrast enhanced MRA technique.<sup>45</sup> Arterial spin labelling techniques can provide non-contrast MRA sequences using an inversion-recovery inflow-based technique.<sup>46</sup> This technique has recently been used to assess the pulmonary vasculature in pre-surgical patients with non-small-cell lung

Figure 3. In this patient with two pulmonary emboli (arrows in panels a and b), the embolus in the right upper lobe (a) looks smaller than the one in the right lower lobe (b) on MR angiography (MRA). However, on time-resolved perfusion MRI, the embolus in the right upper lobe is causing a much larger perfusion defect (\*) (c) than the one in the right lower lobe (d). This suggests that direct assessment of pulmonary function (perfusion in this case) can provide information that is not available on morphologic MRA alone.



cancer<sup>47</sup> and also to look for pulmonary arteriovenous malformations.<sup>48</sup>

### BUILDING A CLINICAL SERVICE

Although the use of pulmonary MRA is increasing, widespread implementation has yet to occur. This is most likely due to a combination of factors, including confidence in the accuracy of CTPA, the quick turnaround time associated with CTPA and the

Figure 4. Axial balanced steady-state free precession: this non-contrast image clearly shows a large central pulmonary embolism within the right main pulmonary artery (solid arrow). Also, a pulmonary infarct within the peripheral lung (dashed arrow) is present.

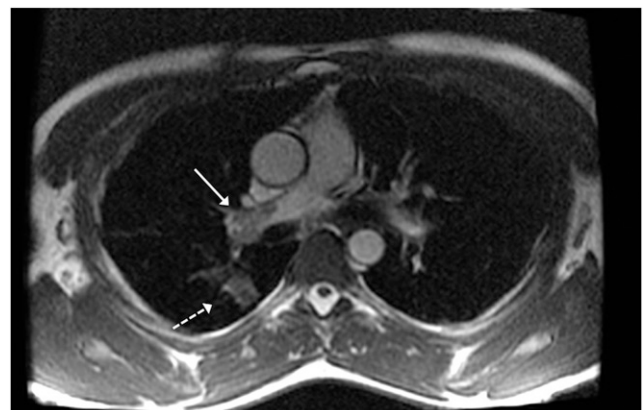
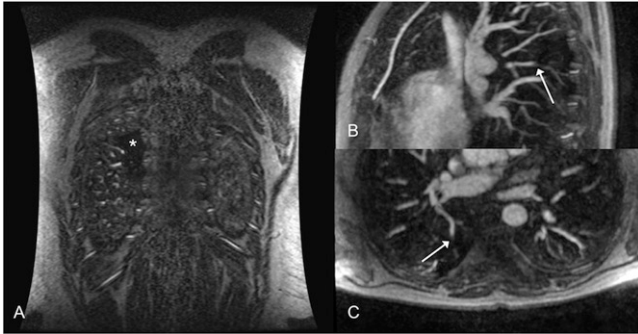




Figure 5. Perfusion defects provide additional information and can focus the search for small subsegmental pulmonary embolism (PE) that may be easily overlooked. (a) Coronal three-dimensional three-dimensional spoiled gradient recalled echo shows a small perfusion defect (asterisk) within the superior segment of the right lower lobe. (b, c) Sagittal and axial reconstructed 5-mm maximum intensity projections show abrupt vascular cut-off of the subsegmental pulmonary artery supplying this area suggesting PE (arrow).



more limited availability of MRI in the emergency department setting. These issues have made it difficult for ordering clinicians to appreciate the advantages of using pulmonary MRA for the primary diagnosis of PE. Educating ordering clinicians about the proper use of and benefits of pulmonary MRA as an alternative to CTPA is very important. It is also important to establish a rapid clinical protocol that can ensure rapid turnaround comparable with CTPA.

CTPA currently remains the standard of care when evaluating for PE, and pulmonary MRA should not replace it in all cases. Pulmonary MRA is an important alternative to CTPA in patients who are younger where the effects of ionizing radiation are of concern. While new iterative reconstruction algorithms have recently been shown to provide acceptable diagnostic performance with CTPA using ultralow radiation doses<sup>49</sup> and may alleviate some of these concerns, these sub-millisievert techniques will require further evaluation before widespread implementation.

Pulmonary MRA is also beneficial in patients with allergies to iodinated contrast and in patients at risk of contrast-induced nephropathy. GBCAs, unlike iodinated contrast agents, are not nephrotoxic. It is also important to consider the overall health status of the patient. Patients who are severely dyspnoeic may be unable to perform adequate breath-holds, making it difficult to perform the pulmonary MRA, which requires a slightly longer breath-hold than CTPA. There is no general consensus on when pulmonary MRA is indicated to evaluate for PE. The PIOPED III authors recommend use only at institutions with adequate experience and only in patients where other examinations are contraindicated.<sup>19,20</sup> The iRefer guidelines provided by the Royal College of Radiologists recommend use when CTPA is contraindicated and ventilation/perfusion scintigraphy is unlikely to be helpful.

An ideal protocol includes a short table time with sequences that can be obtained in a single breath-hold to minimize breathing

motion artefact. The following protocol, which uses techniques described in the previous section, requires only six breath-holds and can be performed with the patient on the scanner for <10 min:<sup>50</sup>

- three-plane single-shot fast spin-echo localizers
- pre-contrast  $T_1$  weighted 3D SGRE
- pulmonary arterial phase  $T_1$  weighted 3D SGRE
- immediate post-contrast  $T_1$  weighted 3D SGRE
- low flip angle post-contrast  $T_1$  weighted 3D SGRE
- $T_1$  weighted 2D axial or 3D SGRE with fat saturation.

The  $T_1$  weighted 3D SGRE acquisition can be reformatted in any plane. For our protocol, coronal reformatted images are saved with additional multiplanar reformatted or maximum intensity projection images created and saved on the workstation, as needed during the interpretation of the study.

To keep the total examination time as short as possible, dedicated perfusion sequences are not part of this protocol. Perfusion defects are commonly seen, however, on the first arterial phase acquisition obtained during the contrast injection.

There are pitfalls that arise in both the acquisition of the pulmonary MRA and in its interpretation. To inspire confidence from ordering physicians, it is crucial that both the technologists and interpreting physician have the experience to provide consistently high-quality images and accurate interpretations in a timely manner. In our experience, however, it does not take long to gain this level of expertise.

At our institution, MRI technologists become comfortable performing pulmonary MRA after just a handful of attempts. One

Figure 6. Axial reconstructed three-dimensional spoiled gradient recalled echo: two apparent filling defects are seen within adjacent right lower lobar segmental pulmonary arteries. The more hypointense central defect is an actual pulmonary embolism (solid arrow) with a drop in signal intensity relative to the surrounding vessel of 69%. The less hypointense central defect is due to Gibbs ringing artefact (dashed arrow) with a drop in signal intensity relative to that of the surrounding vessel of only 20%.

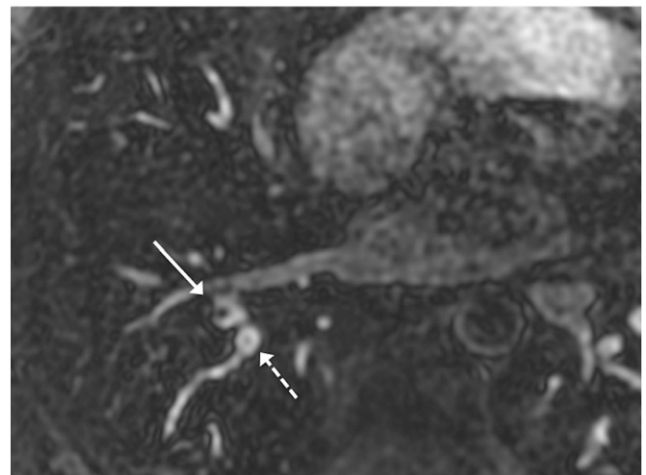
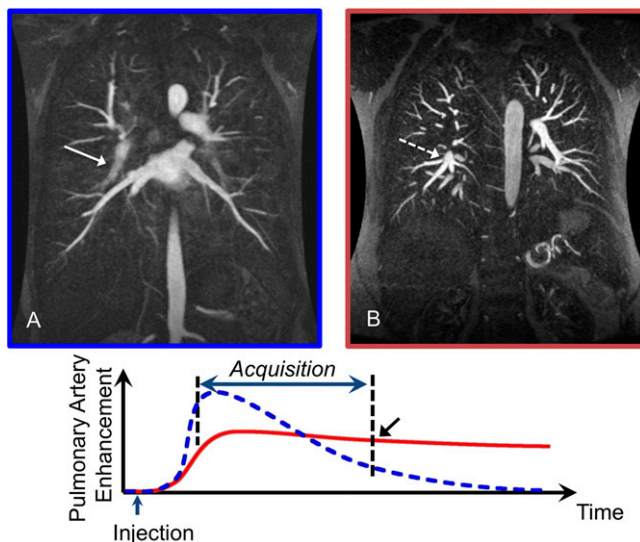


Figure 7. Coronal three-dimensional spoiled gradient recalled echo: the graph demonstrates the different enhancement patterns for a short bolus (dashed curve) compared with a dilute, extended bolus (solid curve). (a) 12 ml of a gadolinium-based contrast agent (GBCA) was injected at a rate of  $1.5 \text{ ml s}^{-1}$  for a total duration of 8 s. This bolus of contrast will give an enhancement pattern similar to the dashed curve on the graph with non-uniform enhancement during the acquisition and relatively little enhancement at the end of the acquisition (black arrow) when the edges of  $k$ -space are sampled. This results in blurring of the arteries (solid arrow). (b) 12 ml of GBCA diluted with saline to a total volume of 30 ml injected at a rate of  $1.5 \text{ ml s}^{-1}$  for a duration of 8 s. The pattern of enhancement corresponds with the solid curve where there is relatively uniform enhancement throughout the acquisition. The edges of  $k$ -space are now sampled when there is still adequate enhancement of the pulmonary arteries resulting in sharp arteries (dashed arrow).



of the greatest challenges is the correct timing of the acquisition relative to the arrival of the contrast bolus. By using a diluted contrast bolus as described above, this is less of a challenge for inexperienced technologists. It is also important for the technologist to communicate effectively with the patient and provide clear breathing instructions to reduce the respiratory artefacts.

## IMAGE INTERPRETATION

The principal imaging findings of PE on pulmonary MRA are similar to those seen on CTPA. A non-occlusive filling defect or a complete occlusion with abrupt vessel cut-off is characteristic of PE (Figure 2). On CTPA, these findings are typically easy to identify and differentiate from the adjacent lung parenchyma. This is not always the case on pulmonary MRA, since an occlusive embolus has the same low signal intensity as the background lung parenchyma. This can obscure even large emboli. It is important for the radiologist to understand the indirect findings on pulmonary MRA that are associated with PE, particularly the presence of perfusion defects, described above, that can be used to guide the search for PE that are not easily identified (Figure 5).

There are several important artefacts that can arise during pulmonary MRA that may be unfamiliar to radiologists who are inexperienced in interpreting pulmonary MRA. The image artefact that causes the most degradation of image quality is respiratory motion artefact. This artefact can only be alleviated by obtaining images when respiratory motion is minimal. Acquiring multiple vascular phases increases the likelihood of obtaining a sequence that has limited motion artefact. In some circumstances, it may be necessary to give an additional dose of contrast and repeat the MRA vascular sequences. Given the lack of ionizing radiation and the high safety profile of GBCAs, a second injection is a feasible method of obtaining a diagnostic examination and is an advantage of MRA over CTPA.

Truncation or Gibbs ringing artefact is the most challenging artefact because it can mimic PE. Most radiologists are familiar with this artefact in the setting of spine MRI, where it can mimic a syrinx within the central cord, or with MRCP with central hypointensity in the common duct that can mimic a stone. This artefact is due to the limited sampling that naturally leads to truncation at the edges of  $k$ -space. This truncation results in ringing or ripples near sharp interfaces such as the edges of an enhancing vessel. This artefact is usually not a diagnostic challenge in most vessels. However, in vessels that are 3–5 pixels in diameter, there is overlap of the ripples from the two vessel edges, leading to a central hypointensity that persists on all vascular phases and can mimic the appearance of an embolus to the inexperienced viewer. This artefact can be differentiated from PE by using the method first described by Bannas et al.<sup>51</sup>

Specifically, they showed that signal drop of  $<50\%$  of the maximum vascular signal was consistent with Gibb's truncation artefact rather than PE (sensitivity 95%, specificity 90%)<sup>51</sup> (Figure 6). There are also artefacts that arise owing to the timing of the centre of  $k$ -space signal acquisition relative to the arrival of the contrast bolus.<sup>52</sup> If the signal acquisition begins before the contrast bolus arrives, there will be edge enhancement, as only the periphery of  $k$ -space is obtained while contrast is present. If the scan begins late during the contrast bolus, there will be blurring of the pulmonary arteries. By diluting the contrast bolus as described previously, the entire  $k$ -space acquisition can be performed while there is a relatively uniform concentration of contrast within the pulmonary arteries (Figure 7).

## FUTURE DIRECTIONS

Ferumoxytol in pulmonary MR angiography  
USPIO contrast agents for performing pulmonary MRA date back to the late 1990s.<sup>53</sup> Ferumoxytol (Feraheme; AMAG ksias) is a USPIO with a carbohydrate coating approved for the treatment of iron deficiency anaemia in patients with chronic kidney disease.<sup>54</sup> The superparamagnetic properties of ferumoxytol shorten the  $T_1$  relaxation time of nearby nuclei, leading to enhancement on  $T_1$  weighted images. On  $T_2^*$  images, there is a loss of signal intensity. The large size of the ferumoxytol molecule relative to extravascular GBCAs allows for very little extravascular leakage, and the carbohydrate coating prevents glomerular filtration. These properties make ferumoxytol an outstanding intravascular contrast agent with

Figure 8. Coronal three-dimensional spoiled gradient recalled echo with axial reconstructions: 3 mg kg<sup>-1</sup> of ferumoxytol was diluted and administered to an 8-week pregnant patient over 15 min: no pulmonary embolus was present. Since the agent is administered as a slow infusion, dynamic images during contrast administration could not be obtained. The post-contrast images are comparable in quality with those obtained with a gadolinium-based contrast agent (compared with Figure 1).



“Post” acquisition - 28° Flip Angle      “Post” acquisition - 15° Flip Angle

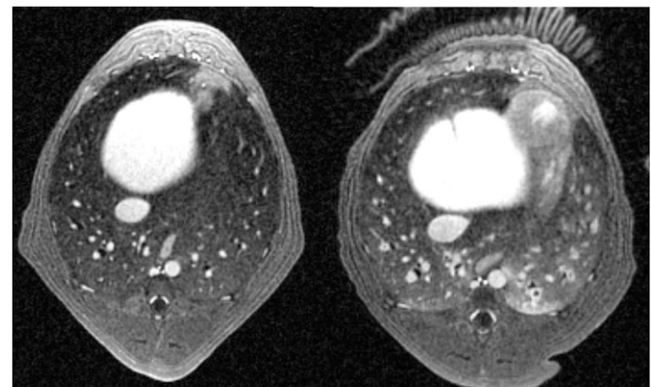
an intravascular residence time of >12 h. Ferumoxytol has been shown to be an effective contrast agent for MRA,<sup>55,56</sup> MR venography<sup>57</sup> and MR lymphangiography.<sup>58</sup> Studies using ferumoxytol appear to be a viable alternative to GBCAs in CE-MRA performed to detect PE (Figure 8), especially in patients with impaired renal function, although no large comparative effectiveness trial has been performed to date. The long intravascular residence time also allows for steady-state imaging that can be used with free breathing techniques.

The use of ferumoxytol as an MRI contrast agent is an off-label application, and extra care should be taken in patient assessment prior to administering the agent. There is a small risk of severe, potentially fatal allergic reactions, particularly in patients with multiple drug allergies.<sup>30</sup> The FDA has issued a black box warning owing to this risk and recommends against a bolus administration.<sup>59</sup> When possible, ferumoxytol should be diluted and administered as an infusion over 15 min.<sup>30</sup> In our experience, the use of a bolus injection of ferumoxytol is not necessary for MRA to detect PE.

#### Ultrashort echo time MRI

Structural lung imaging is challenging owing to the short transverse relaxation times of the lung parenchyma. Recent advances in MRI using ultrashort echo time (UTE) have been utilized to provide high-resolution imaging of lung morphology and to assess for structural lung disease in animals.<sup>60–62</sup> Using radial oversampling, limited field-of-view excitation and variable

Figure 9. Ultrashort echo time (UTE) [echo time (TE) = 0.08 ms] MRI in a dog prior to and following the embolization of the pulmonary arteries enabled simultaneous depiction of small subsegmental pulmonary emboli as well as parenchymal changes of haemorrhage and atelectasis in the left lower lobe. These images were acquired during 5 min of quiet respiration on a ventilator. The clear difference in signal between small bronchi and the adjacent lung shows how UTE methods can be used not only to identify pulmonary emboli but may also be better than conventional TE MRI in depicting alternative diagnoses that may explain the patient symptoms.



Pre-embolization      Post-embolization

readout gradients, 3D radial UTE MRI has provided high-resolution structural imaging of the lungs in human subjects.<sup>63</sup> A recent study applying 3D radial UTE MRI to assess for PE in dogs demonstrated improved image quality compared with conventional pulmonary MRA.<sup>64</sup> 3D radial UTE MRI has also recently been used in dogs to simultaneously acquire pulmonary arterial structure and pulmonary perfusion images during a single acquisition (Figure 9).<sup>65</sup>

#### Pregnant patients

Standard techniques used to evaluate PE, CTPA and nuclear medicine Ventilation/Perfusion ratio scintigraphy expose both the mother and the fetus to ionizing radiation.<sup>66</sup> MRI of pregnant patients and fetal MRI are routinely performed, and there is no known risk to the fetus associated with non-contrast MRI.<sup>67</sup> The administration of GBCAs, on the other hand, is contraindicated in pregnant patients since GBCAs have been shown to cross the placenta<sup>68</sup> and have been observed to be teratogenic at high doses in animal studies.<sup>69</sup> Recent studies have also demonstrated long-term adverse effects of GBCAs on children exposed to GBCAs *in utero*.<sup>70</sup>

Novel non-contrast MRA techniques are increasingly available<sup>71</sup> and may prove beneficial in evaluating for PE in pregnant patients. Sequences such as the bSSFP sequence described above provide a method for assessing for PE without GBCAs. The image quality of bSSFP acquisitions has been shown to be similar to that seen with post-contrast 3D GRE for the central and lobar pulmonary arteries,<sup>41</sup> providing an additional tool without the radiation risks to the mother and fetus associated with CTPA.

Notably, ferumoxytol is widely used to treat iron deficiency anaemia in pregnant patients and is generally considered safe.



No human studies have described the use of ferumoxytol for MRA in pregnant females. Animal studies have shown decreased fetal weights and incidents of fetal malformation but only at doses 13–15 times the typical human dose. These findings place ferumoxytol in the FDA Class C category<sup>72</sup> and use is only recommended in the second and third trimesters and when the benefits outweigh the unknown risks. Thus, ferumoxytol may be an attractive alternative to GBCAs that are contraindicated in pregnancy.

## CONCLUSION

While there are strengths and weaknesses of using contrast-enhanced pulmonary MRA for the primary diagnosis of PE,

there are growing evidence-based outcome data that that MRA is a safe examination for the exclusion of clinically significant PE. In our experience, the utilization of MRA is an accurate, radiation-free imaging test for the primary diagnosis of clinically significant PE.

## FUNDING

The project described was supported by the Clinical and Translational Science Award (CTSA) programme, through the NIH National Center for Advancing Translational Sciences (NCATS), grant UL1TR000427 and KL2TR000428. Additional funding was provided by the National Institute of Diabetes and Digestive and Kidney Diseases, grant K08DK111234 and K24 DK102595.

## REFERENCES

- Sadigh G, Kelly AM, Cronin P. Challenges, controversies, and hot topics in pulmonary embolism imaging. *AJR Am J Roentgenol* 2011; **196**: 497–515.
- CADTH Optimal Use Reports. Optimal strategies for the diagnosis of acute pulmonary embolism: a health technology assessment—project protocol. Ottawa, ON: Canadian Agency for Drugs and Technologies in Health. Copyright (c) 2016 CADTH; 2016.
- Nikolaou K, Thieme S, Sommer W, Johnson T, Reiser MF. Diagnosing pulmonary embolism: new computed tomography applications. *J Thorac Imaging* 2010; **25**: 151–60.
- Carson JL, Kelley MA, Duff A, Weg JG, Fulkerson WJ, Palevsky HL, et al. The clinical course of pulmonary embolism. *N Engl J Med* 1992; **326**: 1240–5. doi: <https://doi.org/10.1056/NEJM199205073261902>
- Stein PD, Fowler SE, Goodman LR, Gottschalk A, Hales CA, Hull RD, et al. Multidetector computed tomography for acute pulmonary embolism. *N Engl J Med* 2006; **354**: 2317–27. doi: <https://doi.org/10.1056/nejmoa052367>
- Brenner DJ, Hall EJ. Computed tomography—an increasing source of radiation exposure. *N Engl J Med* 2007; **357**: 2277–84.
- Hall EJ, Brenner DJ. Cancer risks from diagnostic radiology: the impact of new epidemiological data. *Br J Radiol* 2012; **85**: e1316–17. doi: <https://doi.org/10.1259/bjr/13739950>
- Pearce MS, Salotti JA, Little MP, McHugh K, Lee C, Kim KP, et al. Radiation exposure from CT scans in childhood and subsequent risk of leukaemia and brain tumours: a retrospective cohort study. *Lancet* 2012; **380**: 499–505.
- Mathews JD, Forsythe AV, Brady Z, Butler MW, Goergen SK, Byrnes GB, et al. Cancer risk in 680,000 people exposed to computed tomography scans in childhood or adolescence: data linkage study of 11 million Australians. *BMJ* 2013; **346**: f2360.
- Schiebler ML, Nagle SK, Francois CJ, Replinger MD, Hamedani AG, Vigen KK, et al. Effectiveness of MR angiography for the primary diagnosis of acute pulmonary embolism: clinical outcomes at 3 months and 1 year. *J Magn Reson Imaging* 2013; **38**: 914–25. doi: <https://doi.org/10.1002/jmri.24057>
- Linnet K, Bossuyt PM, Moons KG, Reitsma JB. Quantifying the accuracy of a diagnostic test or marker. *Clin Chem* 2012; **58**: 1292–301.
- Bossuyt PM, Reitsma JB, Linnet K, Moons KG. Beyond diagnostic accuracy: the clinical utility of diagnostic tests. *Clin Chem* 2012; **58**: 1636–43. doi: <https://doi.org/10.1373/clinchem.2012.182576>
- Brismar J, Jacobsson B. Definition of terms used to judge the efficacy of diagnostic tests: a graphic approach. *AJR Am J Roentgenol* 1990; **155**: 621–3.
- Carrier M, Righini M, Wells PS, Perrier A, Anderson DR, Rodger MA, et al. Subsegmental pulmonary embolism diagnosed by computed tomography: incidence and clinical implications. A systematic review and meta-analysis of the management outcome studies. *J Thromb Haemost* 2010; **8**: 1716–22.
- Stein PD, Goodman LR, Hull RD, Dalen JE, Matta F. Diagnosis and management of isolated subsegmental pulmonary embolism: review and assessment of the options. *Clin Appl Thromb Hemost* 2012; **18**: 20–6. doi: <https://doi.org/10.1177/1076029611422363>
- Wiener RS, Schwartz LM, Woloshin S. When a test is too good: how CT pulmonary angiograms find pulmonary emboli that do not need to be found. *BMJ* 2013; **347**: f3368.
- den Exter PL, van Es J, Klok FA, Kroft LJ, Kruij MJ, Kamphuisen PW, et al. Risk profile and clinical outcome of symptomatic subsegmental acute pulmonary embolism. *Blood* 2013; **122**: 1144–19; quiz 329. doi: <https://doi.org/10.1182/blood-2013-04-497545>
- den Exter PL, van Roosmalen MJ, van den Hoven P, Klok FA, Monreal M, Jimenez D, et al. Physicians' management approach to an incidental pulmonary embolism: an international survey. *J Thromb Haemost* 2013; **11**: 208–13.
- Stein PD, Chenevert TL, Fowler SE, Goodman LR, Gottschalk A, Hales CA, et al. Gadolinium-enhanced magnetic resonance angiography for pulmonary embolism: a multicenter prospective study (PIOPED III). *Ann Intern Med* 2010; **152**: 434–43.
- Davidson BL, Lacrampe MJ. Why can't magnetic resonance imaging reliably diagnose pulmonary embolism? *Ann Intern Med* 2010; **152**: 467–8.
- Moore EH, Gamsu G, Webb WR, Stulberg MS. Pulmonary embolus: detection and follow-up using magnetic resonance. *Radiology* 1984; **153**: 471–2. doi: <https://doi.org/10.1148/radiology.153.2.6484180>
- Schiebler ML, Holland GA, Hatabu H, Listerud J, Foo T, Palevsky H, et al. Suspected pulmonary embolism: prospective evaluation with pulmonary MR angiography. *Radiology* 1993; **189**: 125–31. doi: <https://doi.org/10.1148/radiology.189.1.8372181>
- Grist TM, Sostman HD, MacFall JR, Foo TK, Spritzer CE, Witty L, et al. Pulmonary angiography with MR imaging: preliminary clinical experience. *Radiology* 1993; **189**: 523–30. doi: <https://doi.org/10.1148/radiology.189.2.8210385>
- Erdman WA, Peshock RM, Redman HC, Bonte F, Meyerson M, Jayson HT, et al. Pulmonary embolism: comparison of



- MR images with radionuclide and angiographic studies. *Radiology* 1994; **190**: 499–508. doi: <https://doi.org/10.1148/radiology.190.2.8284406>
25. Meaney JF, Weg JG, Chenevert TL, Stafford-Johnson D, Hamilton BH, Prince MR. Diagnosis of pulmonary embolism with magnetic resonance angiography. *N Engl J Med* 1997; **336**: 1422–7. doi: <https://doi.org/10.1056/nejm199705153362004>
  26. Gupta A, Frazer CK, Ferguson JM, Kumar AB, Davis SJ, Fallon MJ, et al. Acute pulmonary embolism: diagnosis with MR angiography. *Radiology* 1999; **210**: 353–9. doi: <https://doi.org/10.1148/radiology.210.2.r99fe53353>
  27. Griswold MA, Jakob PM, Heidemann RM, Nittka M, Jellus V, Wang J, et al. Generalized autocalibrating partially parallel acquisitions (GRAPPA). *Magn Reson Med* 2002; **47**: 1202–10. doi: <https://doi.org/10.1002/mrm.10171>
  28. Brau AC, Beatty PJ, Skare S, Bammer R. Comparison of reconstruction accuracy and efficiency among autocalibrating data-driven parallel imaging methods. *Magn Reson Med* 2008; **59**: 382–95. doi: <https://doi.org/10.1002/mrm.21481>
  29. Londy FJ, Lowe S, Stein PD, Weg JG, Eisner RL, Leeper KV, et al. Comparison of 1.5 and 3.0 T for contrast-enhanced pulmonary magnetic resonance angiography. *Clin Appl Thromb Hemost* 2012; **18**: 134–9. doi: <https://doi.org/10.1177/1076029611419840>
  30. Vasanawala SS, Nguyen KL, Hope MD, Bridges MD, Hope TA, Reeder SB, et al. Safety and technique of ferumoxytol administration for MRI. *Magn Reson Med* 2016; **75**: 2107–11. doi: <https://doi.org/10.1002/mrm.26151>
  31. Finn P. Feraheme as an MRI contrast agent for pediatric congenital heart disease. [updated 22 April 2016; cited 15 November 2016]; Available from: <https://clinicaltrials.gov/show/NCT02752191>
  32. Nguyen KL, Yoshida T, Han F, Ayad I, Reemtsen BL, Salusky IB, et al. MRI with ferumoxytol: a single center experience of safety across the age spectrum. *J Magn Reson Imaging* 2016; **45**: 804–12. doi: <https://doi.org/10.1002/jmri.25412>
  33. Bernstein MA, King KF, Zhou XJ. *Handbook of MRI pulse sequences*. Burlington, MA: Elsevier Academic Press; 2004.
  34. Bernstein MA, Fain SB, Riederer SJ. Effect of windowing and zero-filled reconstruction of MRI data on spatial resolution and acquisition strategy. *J Magn Reson Imaging* 2001; **14**: 270–80. doi: <https://doi.org/10.1002/jmri.1183>
  35. Maxien D, Ingrisch M, Meinel FG, Reiser M, Dietrich O, Nikolaou K. Quantification of pulmonary perfusion with free-breathing dynamic contrast-enhanced MRI—a pilot study in healthy volunteers. *Rofa* 2013; **185**: 1175–81.
  36. Ingrisch M, Maxien D, Schwab F, Reiser MF, Nikolaou K, Dietrich O. Assessment of pulmonary perfusion with breath-hold and free-breathing dynamic contrast-enhanced magnetic resonance imaging: quantification and reproducibility. *Invest Radiol* 2014; **49**: 382–9.
  37. Frechen D, Kruger S, Paetsch I, Kozerke S, Schnackenburg B, Frick M, et al. Pulmonary perfusion imaging: new insights into functional consequences of pulmonary embolism using a multicomponent cardiovascular magnetic resonance imaging protocol. *J Am Coll Cardiol* 2012; **60**: 2335–7.
  38. Ingrisch M, Maxien D, Meinel FG, Reiser MF, Nikolaou K, Dietrich O. Detection of pulmonary embolism with free-breathing dynamic contrast-enhanced MRI. *J Magn Reson Imaging* 2016; **43**: 887–93. doi: <https://doi.org/10.1002/jmri.25050>
  39. Ohno Y, Koyama H, Matsumoto K, Onishi Y, Nogami M, Takenaka D, et al. Dynamic MR perfusion imaging: capability for quantitative assessment of disease extent and prediction of outcome for patients with acute pulmonary thromboembolism. *J Magn Reson Imaging* 2010; **31**: 1081–90. doi: <https://doi.org/10.1002/jmri.22146>
  40. Bell LC, Wang K, Munoz Del Rio A, Grist TM, Fain SB, Nagle SK. Comparison of models and contrast agents for improved signal and signal linearity in dynamic contrast-enhanced pulmonary magnetic resonance imaging. *Invest Radiol* 2015; **50**: 174–8.
  41. Heredia V, Altun E, Ramalho M, de Campos R, Azevedo R, Pamuklar E, et al. MRI of pregnant patients for suspected pulmonary embolism: steady-state free precession vs postgadolinium 3D-GRE. *Acta Med Port* 2012; **25**: 359–67.
  42. Kalb B, Sharma P, Tigges S, Ray GL, Kitajima HD, Costello JR, et al. MR imaging of pulmonary embolism: diagnostic accuracy of contrast-enhanced 3D MR pulmonary angiography, contrast-enhanced low-flip angle 3D GRE, and nonenhanced free-induction FISP sequences. *Radiology* 2012; **263**: 271–8.
  43. Edelman RR, Giri S, Pursnani A, Botelho MP, Li W, Koktzoglou I. Breath-hold imaging of the coronary arteries using Quiescent-Interval Slice-Selective (QISS) magnetic resonance angiography: pilot study at 1.5 Tesla and 3 Tesla. *J Cardiovasc Magn Reson* 2015; **17**: 101.
  44. Swift AJ, Wild JM, Nagle SK, Roldan-Alzate A, Francois CJ, Fain S, et al. Quantitative magnetic resonance imaging of pulmonary hypertension: a practical approach to the current state of the art. *J Thorac Imaging* 2014; **29**: 68–79.
  45. Miyazaki M, Sugiura S, Tateishi F, Wada H, Kassai Y, Abe H. Non-contrast-enhanced MR angiography using 3D ECG-synchronized half-Fourier fast spin echo. *J Magn Reson Imaging* 2000; **12**: 776–83. doi: [https://doi.org/10.1002/1522-2586\(200011\)12:5<776::aid-jmri17>3.0.co;2-x](https://doi.org/10.1002/1522-2586(200011)12:5<776::aid-jmri17>3.0.co;2-x)
  46. Shimada K, Isoda H, Okada T, Maetani Y, Arizono S, Hirokawa Y, et al. Non-contrast-enhanced hepatic MR angiography with true steady-state free-precession and time spatial labeling inversion pulse: optimization of the technique and preliminary results. *Eur J Radiol* 2009; **70**: 111–17.
  47. Ohno Y, Nishio M, Koyama H, Yoshikawa T, Matsumoto S, Seki S, et al. Journal Club: comparison of assessment of preoperative pulmonary vasculature in patients with non-small cell lung cancer by non-contrast- and 4D contrast-enhanced 3-T MR angiography and contrast-enhanced 64-MDCT. *AJR Am J Roentgenol* 2014; **202**: 493–506.
  48. Hamamoto K, Matsuura K, Chiba E, Okochi T, Tanno K, Tanaka O. Feasibility of non-contrast-enhanced MR angiography using the time-SLIP technique for the assessment of pulmonary arteriovenous malformation. *Magn Reson Med Sci* 2016; **15**: 253–65. doi: <https://doi.org/10.2463/mrms.mp.2015-0069>
  49. Sauter A, Koehler T, Fingerle AA, Brendel B, Richter V, Rasper M, et al. Ultra low dose CT pulmonary angiography with iterative reconstruction. *PLoS One* 2016; **11**: e0162716. doi: <https://doi.org/10.1371/journal.pone.0162716>
  50. Nagle SK, Schiebler ML, Repplinger MD, Francois CJ, Vigen KK, Yarlagadda R, et al. Contrast enhanced pulmonary magnetic resonance angiography for pulmonary embolism: building a successful program. *Eur J Radiol* 2016; **85**: 553–63.
  51. Bannas P, Schiebler ML, Motosugi U, Francois CJ, Reeder SB, Nagle SK. Pulmonary MRA: differentiation of pulmonary embolism from truncation artefact. *Eur Radiol* 2014; **24**: 1942–9.
  52. Maki JH, Prince MR, Londy FJ, Chenevert TL. The effects of time varying intravascular signal intensity and *k*-space acquisition order on three-dimensional MR angiography image quality. *J Magn Reson Imaging* 1996; **6**: 642–51. doi: <https://doi.org/10.1002/jmri.1880060413>
  53. Ahlstrom KH, Johansson LO, Rodenburg JB, Ragnarsson AS, Akeson P, Borseth A.

- Pulmonary MR angiography with ultrasmall superparamagnetic iron oxide particles as a blood pool agent and a navigator echo for respiratory gating: pilot study. *Radiology* 1999; **211**: 865–9.
54. Spinowitz BS, Kausz AT, Baptista J, Noble SD, Sothinathan R, Bernardo MV, et al. Ferumoxylol for treating iron deficiency anemia in CKD. *J Am Soc Nephrol* 2008; **19**: 1599–605. doi: <https://doi.org/10.1681/ASN.2007101156>
  55. Hope MD, Hope TA, Zhu C, Faraji F, Haraldsson H, Ordovas KG, et al. Vascular imaging with ferumoxylol as a contrast agent. *AJR Am J Roentgenol* 2015; **205**: W366–73. doi: <https://doi.org/10.2214/AJR.15.14534>
  56. Bashir MR, Bhatti L, Marin D, Nelson RC. Emerging applications for ferumoxylol as a contrast agent in MRI. *J Magn Reson Imaging* 2015; **41**: 884–98. doi: <https://doi.org/10.1002/jmri.24691>
  57. Bashir MR, Mody R, Neville A, Javan R, Seaman D, Kim CY, et al. Retrospective assessment of the utility of an iron-based agent for contrast-enhanced magnetic resonance venography in patients with endstage renal diseases. *J Magn Reson Imaging* 2014; **40**: 113–18. doi: <https://doi.org/10.1002/jmri.24330>
  58. Maki JH, Neligan PC, Briller N, Mitsumori LM, Wilson GJ. Dark blood magnetic resonance lymphangiography using dual-agent relaxivity contrast (DARC-MRL): a novel method combining gadolinium and iron contrast agents. *Curr Probl Diagn Radiol* 2016; **45**: 174–9.
  59. Food and Drug Administration. FDA Drug Safety Communication: FDA strengthens warnings and changes prescribing instructions to decrease the risk of serious allergic reactions with anemia drug Feraheme (ferumoxylol). [updated 30 March 2015; cited 28 November 2016]; Available from: <http://www.fda.gov/Drugs/DrugSafety/ucm440138.htm>
  60. Togao O, Ohno Y, Dimitrov I, Hsia CC, Takahashi M. Ventilation/perfusion imaging of the lung using ultra-short echo time (UTE) MRI in an animal model of pulmonary embolism. *J Magn Reson Imaging* 2011; **34**: 539–46. doi: <https://doi.org/10.1002/jmri.22645>
  61. Zurek M, Bessaad A, Cieslar K, Cremillieux Y. Validation of simple and robust protocols for high-resolution lung proton MRI in mice. *Magn Reson Med* 2010; **64**: 401–7. doi: <https://doi.org/10.1002/mrm.22360>
  62. Togao O, Tsuji R, Ohno Y, Dimitrov I, Takahashi M. Ultrashort echo time (UTE) MRI of the lung: assessment of tissue density in the lung parenchyma. *Magn Reson Med* 2010; **64**: 1491–8. doi: <https://doi.org/10.1002/mrm.22521>
  63. Johnson KM, Fain SB, Schiebler ML, Nagle S. Optimized 3D ultrashort echo time pulmonary MRI. *Magn Reson Med* 2013; **70**: 1241–50. doi: <https://doi.org/10.1002/mrm.24570>
  64. Bannas P, Bell LC, Johnson KM, Schiebler ML, Francois CJ, Motosugi U, et al. Pulmonary embolism detection with three-dimensional ultrashort echo time MR imaging: experimental study in canines. *Radiology* 2016; **278**: 413–21. doi: <https://doi.org/10.1148/radiol.2015150606>
  65. Bell LC, Johnson KM, Fain SB, Wentland A, Drees R, Johnson RA, et al. Simultaneous MRI of lung structure and perfusion in a single breathhold. *J Magn Reson Imaging* 2015; **41**: 52–9. doi: <https://doi.org/10.1002/jmri.24520>
  66. Revel MP, Cohen S, Sanchez O, Collignon MA, Thiam R, Redheuil A, et al. Pulmonary embolism during pregnancy: diagnosis with lung scintigraphy or CT angiography? *Radiology* 2011; **258**: 590–8. doi: <https://doi.org/10.1148/radiol.10100986>
  67. Nagayama M, Watanabe Y, Okumura A, Amoh Y, Nakashita S, Dodo Y. Fast MR imaging in obstetrics. *Radiographics* 2002; **22**: 563–80; discussion 80–2. doi: <https://doi.org/10.1148/radiographics.22.3.g02ma03563>
  68. Shellock FG, Kanal E. Safety of magnetic resonance imaging contrast agents. *J Magn Reson Imaging* 1999; **10**: 477–84. doi: [https://doi.org/10.1002/\(sici\)1522-2586\(199909\)10:3<477::aid-jmri33>3.3.co;2-5](https://doi.org/10.1002/(sici)1522-2586(199909)10:3<477::aid-jmri33>3.3.co;2-5)
  69. Okuda Y, Sagami F, Tirono P, Morisetti A, Bussi S, Masters RE. Reproductive and developmental toxicity study of gadobenate dimeglumine formulation (E7155) (3)—study of embryo-fetal toxicity in rabbits by intravenous administration. *J Toxicol Sci* 1999; **24**(Suppl. 1): 79–87.
  70. Ray JG, Vermeulen MJ, Bharatha A, Montanera WJ, Park AL. Association between MRI exposure during pregnancy and fetal and childhood outcomes. *JAMA* 2016; **316**: 952–61.
  71. Miyazaki M, Akahane M. Non-contrast enhanced MR angiography: established techniques. *J Magn Reson Imaging* 2012; **35**: 1–19. doi: <https://doi.org/10.1002/jmri.22789>
  72. Food and Drug Administration. Feraheme package insert. [Cited 28 November 2016]; Available from: [http://www.accessdata.fda.gov/drugsatfda\\_docs/label/2009/022180lbl.pdf](http://www.accessdata.fda.gov/drugsatfda_docs/label/2009/022180lbl.pdf)